Geomechanics and Engineering, *Vol. 21, No. 4 (2020) 315-326*
DOI: https://doi.org/10.12989/gae.2020.21.4.315

Effect of particle size and saturation conditions on the breakage factor of weak rockfill materials under one-dimensional compression testing

Hamidreza Rahmani[a] and Ali Komak Panah*

Faculty of Civil and Environmental Engineering, Tarbiat Modares University, Tehran, Iran

(Received July 16, 2019, Revised March 16, 2020, Accepted March 20, 2020)

Abstract. The long-term behavior of rockfill material used in the construction of infrastructures such as dams is of great significance. Because of concerns about the application of weak rockfill material in dam construction, further experimental studies on the behavior of these materials are required. In this study, laboratory experiments were performed to investigate the one-dimensional deformation and particle breakage of the weak rockfill material under stress. A one-dimensional compression apparatus was designed and developed for testing of rockfill materials of different maximum particle sizes (MPSs). The compression tests were performed under dry, wet and saturated conditions on samples of rockfill material obtained from a dam construction site in Iran. The results of the experiments conducted at the specimen preparation stage and the 1D compression tests are presented. In weak rockfill, the effect of the addition of water on the behavior of the material was uncertain as there were both an increases and decreases observed in particle breakage. Increasing the MPS of the weak rockfill materials increased particle breakage, which was similar to the behavior of strong rockfill material. In all of the MPSs examined, the settlement of specimens under wet conditions was higher than that observed under dry conditions. Also, the greatest deformation occurred during the first hour of loading.

Keywords: particle breakage; weak rockfill material; 1D compression test

1. Introduction

Rockfill material has been extensively used in the construction of dams in the past 150 years (Galloway 1939, Cooke 1984, 1993). Laboratory experiments on rockfill material that are designed to determine their compressibility are inherently difficult due to limitations in the particle size for the testing equipment and the difficulty of modeling the segregation and differential compaction of the layers.

Rockfill shows significant time-dependent behavior. Continuous settlement has been recorded in rockfill dams many decades after construction (Marsal *et al.* 1965, Sowers *et al.* 1965, Sherard and Cooke 1987). Among the five factors (particle breakage, confining pressure, initial void ratio, maximum particle size, coefficient of uniformity), the confining pressure and particle breakage index play the most important roles in determining the strength of rockfill materials (Marsal *et al.* 1965, Marsal 1967, Marachi *et al.* 1972, Indraratna *et al.* 1993, Varadarajan *et al.* 2003, Xiao *et al.* 2016).

The particle breakage index quantifies the degree of particle breakage and can reflect the degree of crushing of the particles in rockfill material and, thus, its energy dissipation. The particle breakage index can be divided into different categories using the following methods: (i) particle size distribution (PSD) methods such as B_g (Marsal 1967), B_r (Hardin 1985), and B_{10} (Lade *et al.* 1996); (ii) the fines content method (Miura *et al.* 2003); (iii) the area method (Miura and Yamamoto 1976; Cristian 2011) and; (iv) the discrete element method (DEM) (Einav *et al.* 2007, Ben-Nun and Einav 2010, Khalkhali *et al.* 2011).

Particle breakage index B_g (Marsal 1967) increases as the confining pressure increases and decreases as the coefficient of uniformity (C_u) increases. There are no obvious variations in B_g at different initial void ratios or for materials having the MPS (Marsal *et al.* 1965, Marsal 1967, Marachi *et al.* 1972, Charles and Watts 1980, Indraratna *et al.* 1993, Varadarajan *et al.* 2003, Xiao *et al.* 2016).

Experimental research is one of the most effective ways to investigate the grain crushing characteristics of granular soil. These include single-particle crushing tests, 1D compression tests, large-scale triaxial tests, plane strain tests and multiaxial tests (Xiao *et al.* 2018). One commonly used experiment on rockfill material is the 1D compression test, because it is more available than large-scale triaxial tests.

Parkin (1977) studied three aspects of the compression behavior of rockfill: load-deformation, time-settlement, and saturation behaviors. Nishiyama *et al.* (2006) evaluated the durability of rockfill materials for dams using the compressive yield stress as measured by 1D compression testing. Neves and Veiga Pinto (1988) presented a method for modelling the collapse of rockfill dams using 1D compression tests.

Nakata *et al.* (2001) investigated the relation between the 1D compression behavior of uniformly graded sand and

*Corresponding author, Associate Professor
E-mail: a-panah@modares.ac.ir
[a]Ph.D. Candidate

http://www.techno-press.org/?journal=gae&subpage=7
ISSN: 2005-307X (Print), 2092-6219 (Online)

single-particle crushing strength and defined five modes for grain crushing in 1D compression tests: (i) no visible damage; (ii) single abrasion; (iii) more than one asperity fracture; (iv) major splitting and; (v) further crushing of sub-particles. Similar research was done by Yamamuro *et al.* (1996) and Xiao *et al.* (2018).

Oldecop and Alonso (2007) performed large diameter oedometer tests to examine the long-term strain in compacted gravel and found that there is a linear relationship between long-term strain and logarithmic time. Zhang *et al.* (2012) portrayed the evolution of the PSD for argillaceous siltstone material subjected to stress and three types of weathering.

Researchers have identified the elastic and shear strength parameters of modeled rockfill materials using large-scale triaxial tests (Gupta 2009, Vasistha *et al.* 2013, Honkanadavar and Sharma 2016). Some have shown that the stress-strain and strength characteristics of rockfill material depend on particle breakage (Gupta 2000, Araei *et al.* 2012a, b, Vasistha *et al.* 2012, Xiao *et al.* 2014, Xiao 2017). Gupta (2009, 2016) showed that the breakage factor for alluvial and blasted rockfill materials increased as the particle size increased. Researchers have also reported a significant decrease in the strength of weathered soft rock (Cetin *et al.* 2000, Sayao *et al.* 2005, Oldcop and Alonso 2007, Woo *et al.* 2010, Miscevic and Vlastelica 2009, Zhang *et al.* 2012, Zhang *et al.* 2015, Yin *et al.* 2016).

Weak rockfill material constitutes more than half of the rocks exposed at or just below the earth surface. As a result, investigation of the behavior of weak rock used in large structures such as rockfill dams is of great significance. Few studies have been carried out to date that investigate the particle breakage behavior of weak rockfill materials; thus, systematic investigation of the mechanical characteristics of weak rockfill materials, particularly particle breakage, is essential.

In the present experimental study, 1D compression tests are carried out to investigate the behavior of weak rockfill materials. The results of the experiments were used to monitor the breakage factor and settlement of weak rockfill materials. The effects of particle size and saturation conditions on the breakage factor and settlement of weak rockfill materials also are investigated.

2. Test apparatus and materials

A 1D compression test apparatus was designed and manufactured for this study in accordance with ICOLD (1993), Nobari and Duncan (1972), Sowers *et al.* (1965), Parkin (1977), Nishiyama *et al.* (2006), Neves and Veiga Pinto (1988), Nakata et al (2001), Yamamuro *et al.* (1996), and Xiao *et al.* (2018) (Fig. 1).

The testing apparatus was composed of the following parts as specified in Fig. 1:

1. Cylinder and compression jack with a full capacity of 100 tons.

2. Steel frame of 70 cm in width and with a variable height of 70-150 cm. The plan dimensions of the steel frame were 70×100 cm.

3. The cell was shaped like a standard oedometer cell and could accommodate specimens of 30 cm in diameter and 50 cm in height. Water could drain from both the top and bottom of the rockfill samples.

Fig. 1 1D compression test apparatus

4. The hydraulic accumulator was charged with nitrogen gas. This was a pressure storage reservoir in which non-compressible hydraulic fluid was held under pressure from an external source. The source could be a spring, raised weight, or compressed gas. The accumulator enabled the hydraulic system to cope with extreme demand while using a less powerful pump. It was able to respond more quickly to a temporary demand and also smooth out the pulsations. A hydraulic accumulator can be considered to be an energy storage device.

5. A de-aired water tank for use in the saturation tests.

6. A pressure sensor with a capacity of 60 MPa.

7. Two linear variable differential transducers (LVDTs) that are connected to the data logger to monitor the displacement during the experiments.

Los Angeles tests also were carried out on the rockfill materials in this study. The Los Angeles test is usually conducted to determine the abrasion resistance of materials. Abrasion resistance seems to be closely related to other resistance properties of rock, particularly particle breakage. It is easy to access a Los Angeles abrasion test apparatus; thus, if the findings of the 1D compression test and Los Angeles test can be related, the results of the Los Angeles test can be used to estimate other parameters. In this study, Los Angeles abrasion tests were performed using the standard test method for resistance to degradation by abrasion and impact of large-sized coarse aggregate in the Los Angeles machine (ASTM C535 2003) in order to investigate the particle breakage of the rockfill material. A 10-kg sample of the material, which was prepared for the 1D compression tests at various particle sizes, was used for the Los Angeles experiment.

As mentioned, the current study focused on the behavior of weak rockfill materials. Samples from different provinces of Iran were sought for the experiments and the Nohob dam site ultimately was selected because of the diversity of its weak rock mines. Nohob dam is a rockfill dam under construction to the southwest of the city of Takestan in Qazvin province (Fig. 2). It is located in an important area of the Kharroud river that is now under development (Absaran 2010).

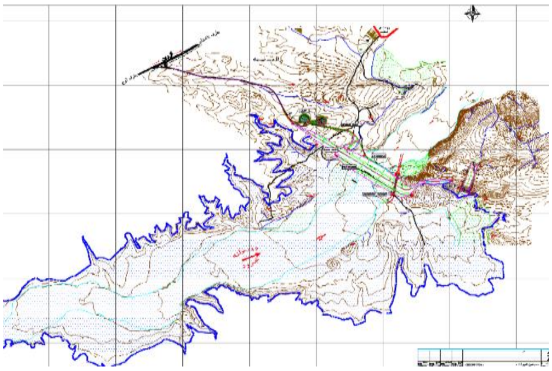

Fig. 2 Nohob storage dam

Table 1 UCS of samples from different sections

Sampling location	Uniaxial compressive strength (MPa)
Spillway 1	23.5
Spillway 2	45.5
Spillway 3	80.4
Spillway 4	26.3
Quarry A	12.6
Quarry D	15.5

Table 2 Strength classification of rock (ICOLD 1993, 2008)

Class	Description	Uniaxial compressive strength (MN/m^2)
A	Very high strength	Over 200
B	High strength	100 – 200
C	Medium strength	50 – 100
D	Low strength	25 – 50
E	Very low strength	Less than 25

Fig. 3 Sampling site

The application of rockfill material from spillway excavation and other rockfill quarries in the area of Nohob dam lacked conviction. As a result, sampling was done to study the applicability of the such materials for the dam body. Uniaxial compressive strength (UCS) (ISRM 2000) tests were performed on the samples and the results are presented in Table 1.

Table 2 presents the ICOLD classifications of rockfill materials based on UCS. As shown, classes C, D, E are

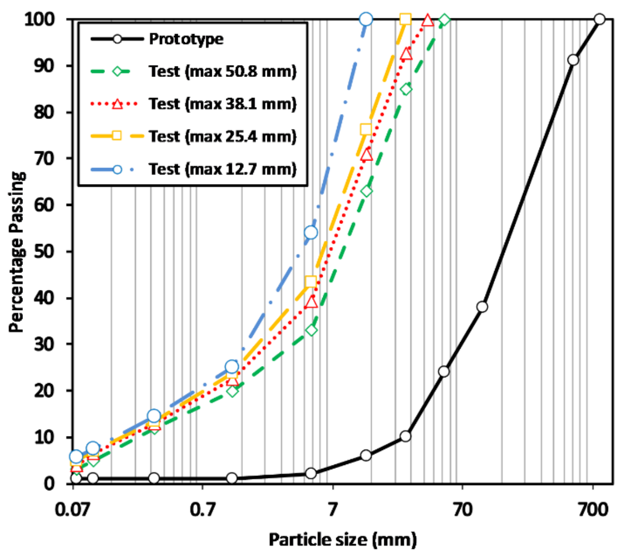

Fig. 4 Gradation of material

considered to be weak rockfill (ICOLD 1993, 2008).

Samples obtained from the foundation excavation of spillways 1 and 2 fell into classes D and E of Table 2 and were selected for the subsequent experiments. These samples were examined in the Rock Mechanics Laboratory to determine their rock geology type. Spillway 1 material was in the dacite category and spillway 2 material was in the andesite rock category. Next, the rockfill materials were sampled for grading. Fig. 3 demonstrates sampling at the dam site.

The mean grain size distribution curve was for this study was derived from grain size distribution curves of quarried rockfill materials used for construction of rockfill dams in different regions of the world (Fig. 4). The diameter of the test cell was 30 cm and the maximum cell-to-grain size ratio was $D/d = 6$ where D and d are the diameter of the test cell and the maximum grain size of the sample, respectively. Fig. 4 shows a model of the rockfill materials for MPSs of 50.8, 38.1, 25.4 and 12.7 mm that were obtained using the parallel gradation technique (Lowe 1964).

Standard test methods for the maximum index density and unit weight of soil using a vibratory table and minimum index density and unit weight of soil (ASTM D4253 2016 and ASTM D4254 2016) were used to determine the maximum and minimum dry unit weight of materials and calculate the relative densities. Subsequently, maximum dry unit weight$(\gamma_d)_{max}$was determined as the ratio of the total weight of the material in the mold to the total volume of the mold occupied by the material. Table 3 lists the results of these experiments.

Based on $(\gamma_d)_{min}$ and $(\gamma_d)_{max}$ of the material at a relative density for the specimens of 87%:

$$RD = \frac{\frac{1}{(\gamma_d)_{min}} - \frac{1}{\gamma_d}}{\frac{1}{(\gamma_d)_{min}} - \frac{1}{(\gamma_d)_{max}}} \times 100\% \tag{1}$$

where γ_d is the dry unit weight under a given condition and $(\gamma_d)_{max}$ and $(\gamma_d)_{min}$ are the maximum and

Table 3 Maximum and minimum density

Material	d_{max} (mm)	γ_d $({}^{kg}/{}_{m^3})$	
		Max	Min
Dacite	12.7	1575	1465
	25.4	1585	1470
	38.1	1603	1480
	50.8	1612	1485
Andesite	12.7	1830	1730
	25.4	1865	1745
	38.1	1880	1760
	50.8	1890	1770

Table 4 Material unit weight in tests

Material	d_{max} (mm)	γ_d $({}^{kg}/{}_{m^3})$
Dacite	12.7	1560
	25.4	1570
	38.1	1587
	50.8	1595
Andesite	12.7	1817
	25.4	1849
	38.1	1864
	50.8	1874

minimum dry unit weights, respectively. Table 4 lists the results of these experiments.

3. Testing program and procedure

The 1D compression tests were performed under the following conditions:

A. Dry condition: The dry materials were placed in the cell, compacted and vertical loading was applied.

B. Wet condition: The wet materials were placed in the cell, compacted and vertical loading was applied. After placing the sample in the cell, the cell valves were opened to allow the free water to drain as stress is applied to the sample.

C. Saturated after dry condition: The sample was prepared and initial loading was applied as done in the dry condition.

D. Saturated after wet condition: The sample was prepared and initial loading was applied as done in the wet condition.

In the wet condition, ASTM D 2216 was used to define the water content. The test samples were prepared in five layers and the water content was measured in each layer. The average water content of the layers was considered to be the sample water content and, in the experiments, the difference between the measured moisture content and the expected moisture content (20%) was ±1%.

In tests C and D, following the completion of the initial loading steps, loading remained unchanged and the bottom valve of the cell was opened. Next, water was injected into the sample from the de-aired water tank (input water) and water was removed from the top of the cell (output water). When the volume of the input and the output water were equal, the bottom valve of the cell was closed and maximum stress was applied to the sample for seven days. Table 5 shows the details of 1D compression tests conducted on the rockfill materials. The saturation is dam impounding equivalent in accordance with ICOLD (1993), Nobari and Duncan (1972), and Neves *et al.* (1989), who used this method to saturate 1D compressive samples. Seven days were required for the sample to be completely saturated.

Table 5 Details of 1D compression tests

Materials	Test conditions	d_{max} (mm)
Dacite, Andesite	Dry condition	12.7, 25.4, 38.1, 50.8
	Wet condition	12.7, 25.4, 38.1, 50.8
	Saturated after dry condition	12.7, 25.4, 38.1, 50.8
	Saturated after wet condition	12.7, 25.4, 38.1, 50.8

Fig. 5 Compaction method used to prepare specimens

Table 6 Vertical stress vs. days of loading

Day	Vertical stress (kPa)	
	Dacite	Andesite
1	320	375
2	640	750
3	960	1125
4	1280	1500
5	1600	1875
6	1920	2250
7	2240	2625

In order to reduce side friction between the specimens and cell, a lubricant was applied to the inner wall of the container prior to placement of the specimen. The rockfill materials were compacted in the container in five lifts. The MPS at each lift was maintained for about half the thickness of the lift. Fig. 5 shows the use of the electric hammer to compact the materials and prepare the specimens.

Volumetric (vertical) deformation of the specimens during tested was monitored using the LVDTs installed at

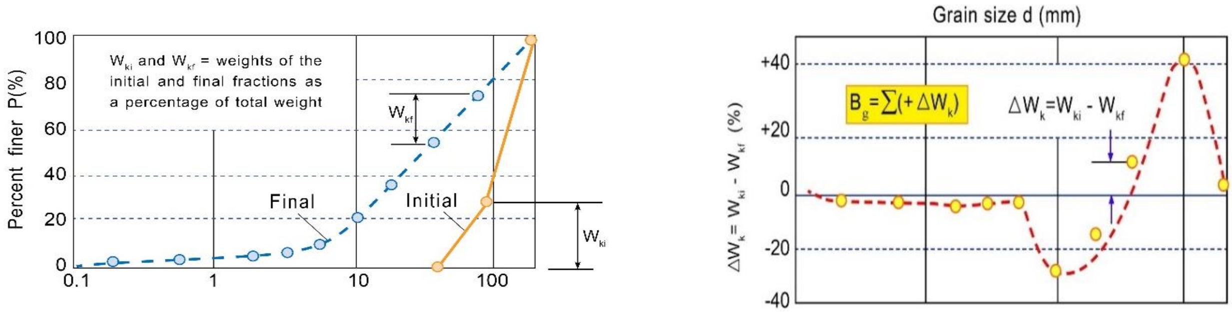

Fig. 6 Quantitative measure of particle breakage

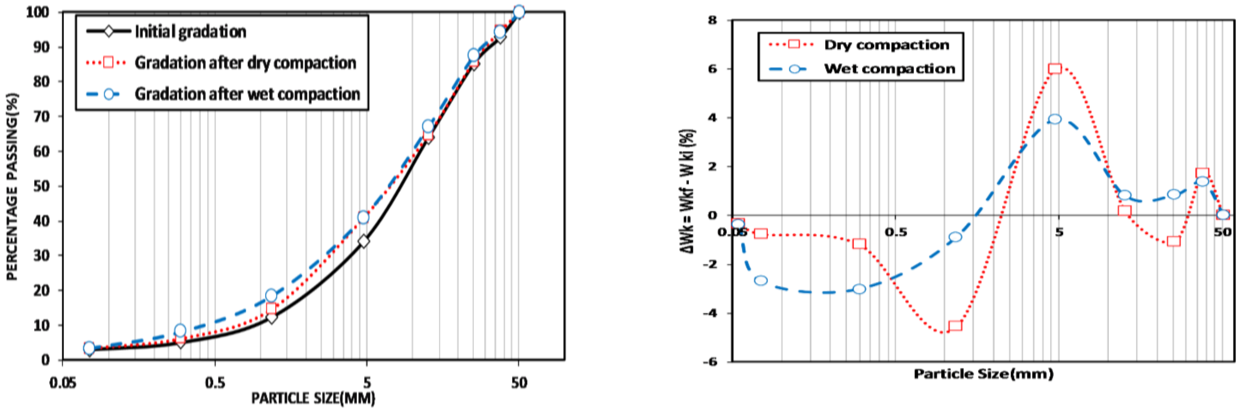

(a) Gradation after compaction (b) ΔW_k after compaction

Fig. 7 Dacite material ($d_{max} = 50.8$ mm)

the top of the specimen. In this study, the vertical stress applied to the specimen was considered to be the loading applied to the specimen. Loading was applied in seven steps of 24 h in duration. The loading was increased at the end of each step. Table 6 lists the loading applied to the dacite and andesite materials according to the day applied.

The 1D compression tests were performed on the rockfill materials to provide quantitative evaluation of particle breakage during loading of the specimens. After each experiment, a sieve analysis test was carried out to obtain the grain size distribution curve.

4. Test results

Marsal (1967) used triaxial test results to define a quantitative measure of particle breakage (Fig. 6). The difference between the grain size fraction before and after the test can be determined as follows:

$$\Delta W_k(\%) = W_{ki} - W_{kf} \tag{2}$$

where W_{ki} and W_{kf} are the grain size fractions before and after the triaxial test, respectively. Afterwards, B_g was defined as the sum of the positive ΔW_k, which is the percentage by weight of the solid phase that has undergone breakage.

Breakage B_g was estimated using the results of grain size distribution tests performed prior to and following the triaxial tests. Fig. 6 shows the evolution of the PSD curve in the tests. The difference between a grain size fraction before and after the triaxial test (ΔW_k) was calculated based on the PSD after the specimen was prepared.

4.1 Particle breakage

4.1.1 Particle breakage during specimen preparation

Significant particle breakage occurred due to compaction during specimen preparation. Fig. 7(a) shows the PSD curve for dacite ($d_{max} = 50.8$ mm) before and after compaction during specimen preparation under both dry and wet conditions and Fig. 7(b) shows the ΔW_k on different sieves. Table 7 shows the values of B_g for dacite

Table 7 B_g values after specimen preparation

Material	d_{max} (mm)	B_g	
		Dry tests	Wet tests
Dacite	12.7	3.74	3.41
	25.4	5.66	4.97
	38.1	6.93	6.09
	50.8	7.91	6.96
Andesite	12.7	2.92	3.34
	25.4	3.37	4.01
	38.1	3.97	4.89
	50.8	5.17	5.96

and andesite specimens prepared under dry and wet conditions.

It can be seen in Table 7 that an increase in d_{max} increased particle breakage for both types of material under dry and wet conditions. Furthermore, for the dacite specimens, the addition of water decreased particle

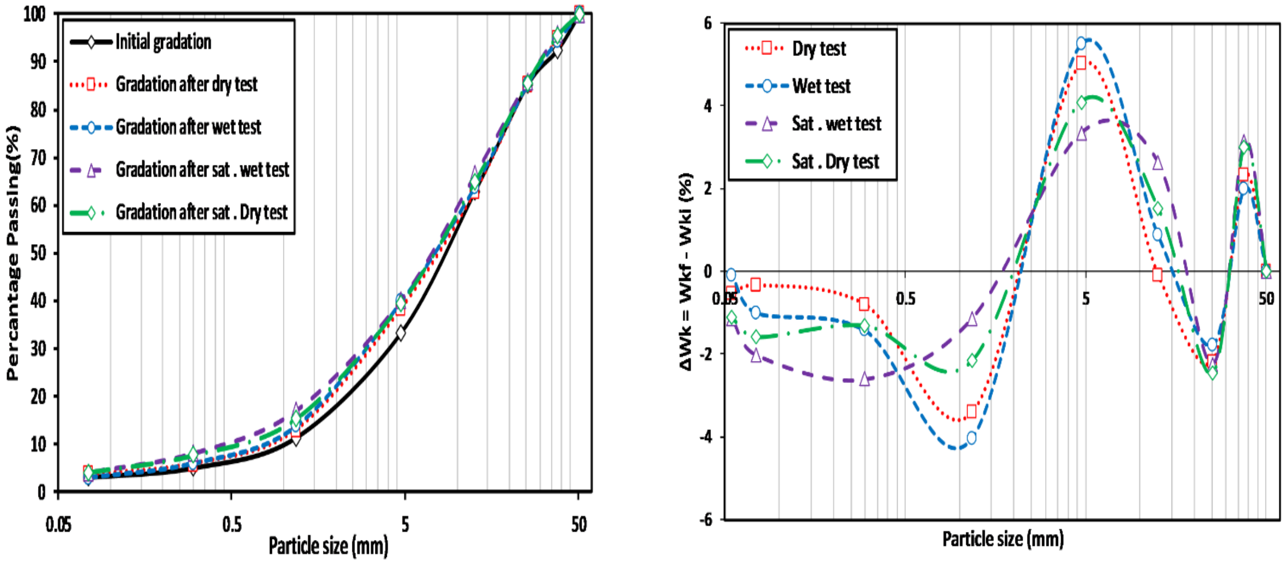

(a) Gradation after 1D compression tests (b) Values of ΔW_k after 1D compression tests

Fig. 8 Andesite specimens (d_{max} = 50.8 mm)

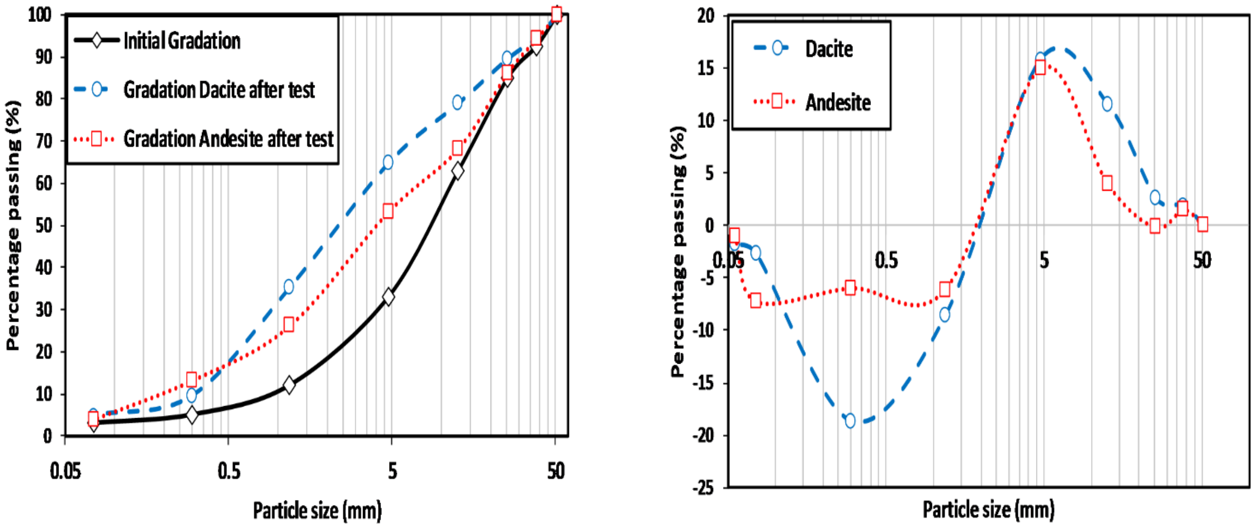

(a) Gradation after Los Angeles tests (b) Values of ΔW_k after Los Angeles tests

Fig. 9 Dacite and andesite specimens (d_{max} = 50.8 mm)

Table 8 B_g after 1D compression tests

Material	d_{max} (mm)	Test conditions			
		Dry	Wet	Sat after dry	Sat after wet
Dacite	12.7	5.35	5.23	5.78	5.61
	25.4	7.44	7.01	7.91	7.63
	38.1	8.97	8.39	9.57	9.1
	50.8	11.68	11.21	12.2	12.04
Andesite	12.7	3.52	3.99	4.01	4.31
	25.4	4.54	5.14	5.26	5.61
	38.1	5.35	6.07	6.23	6.62
	50.8	7.35	8.32	8.64	9.12

breakage at the specimen preparation stage. For the andesite specimens, there was an increase in particle breakage at the same stage with the of addition water.

Table 9 B_g after Los Angeles tests

Material	d_{max} (mm)			
	12.7	25.4	38.1	50.8
Dacite	15.06	24.13	25.41	31.75
Andesite	11.77	17.1	20.59	20.46

4.1.2 Particle breakage after 1D compression tests

Particle breakage occurred in the materials during the 1D compression tests and loading processes. The PSD curve of the andesite (d_{max} = 50.8 mm) before compaction and after 1D compression testing under dry, wet and saturated conditions are shown in Fig. 8(a).

Fig. 8(b) show ΔW_k on different sieves for andesite specimens(d_{max} = 50.8 mm) before and after 1D compression tests under dry, wet and saturated conditions.

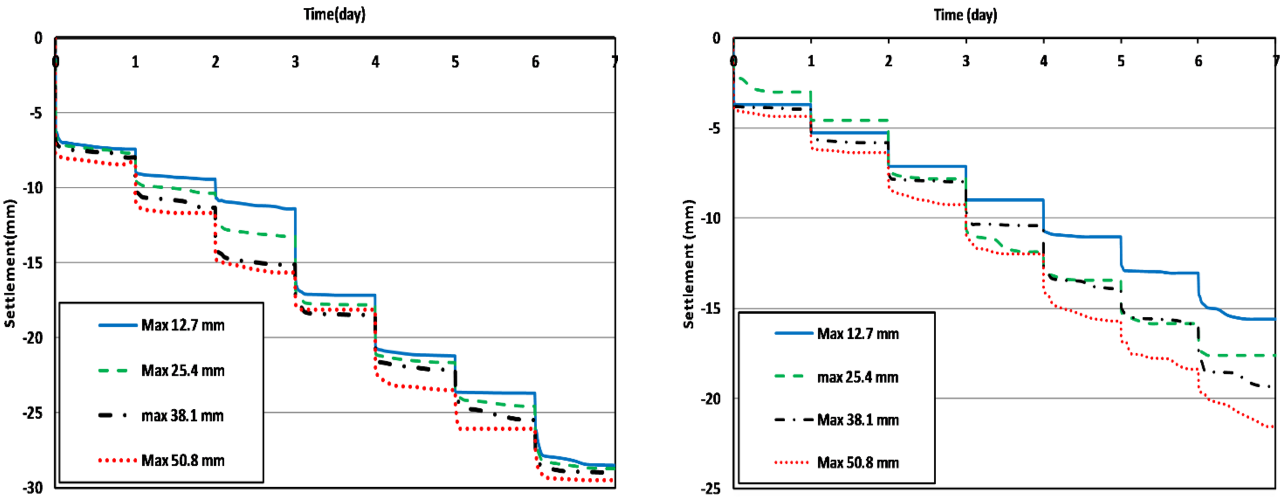

(a) Dacite material under wet conditions (b) Andesite material under dry conditions

Fig. 10 Settlement for 1D compressional test at different values of d_{max}

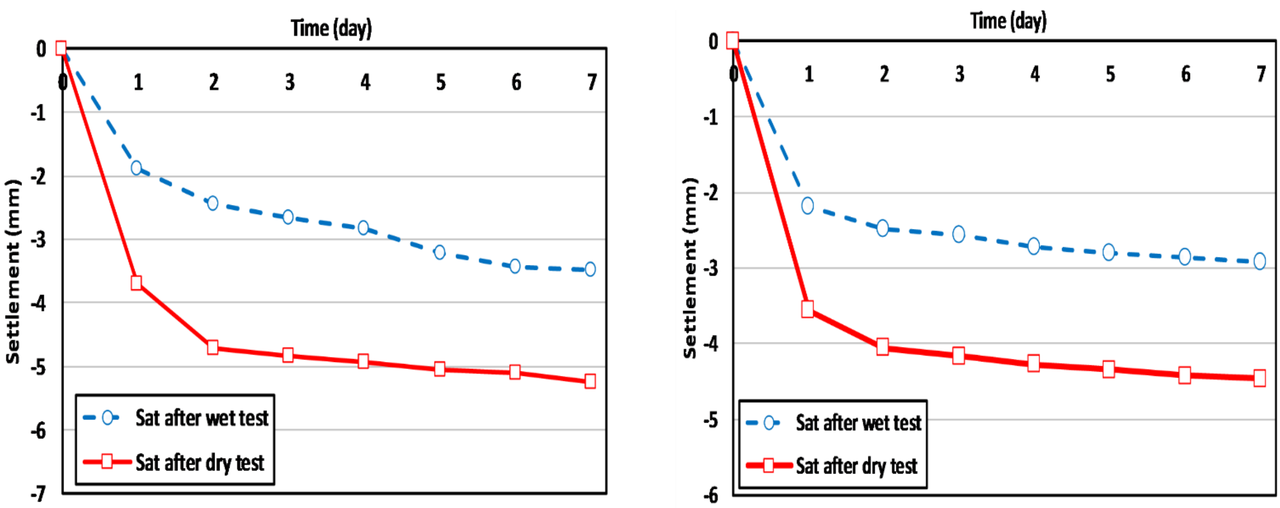

(a) Dacite material (b) Andesite material

Fig. 11 Settlement for 1D compression test under saturated condition (d_{max} = 50.8 mm)

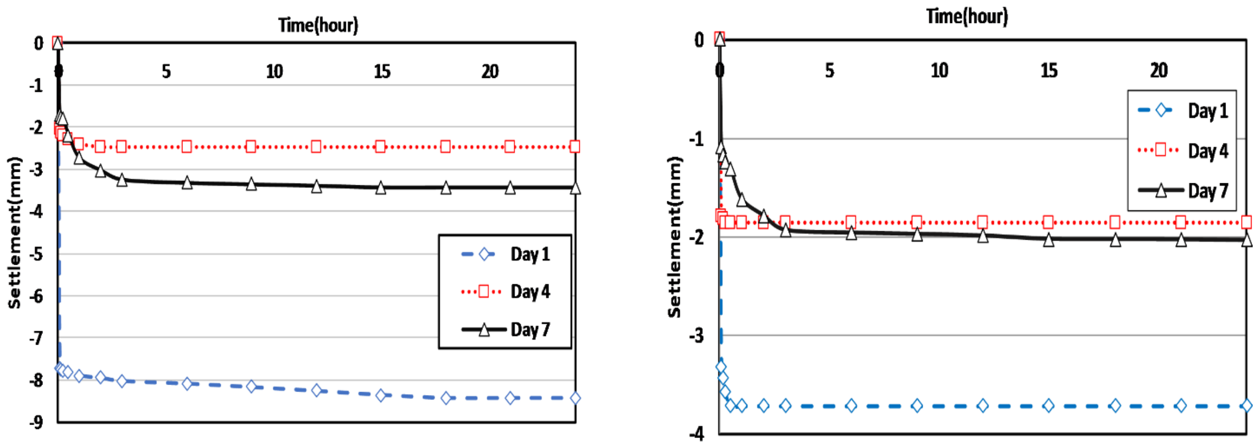

(a) Dacite material under wet conditions (b) Andesite material under dry condition

Fig. 12 Settlement during 1D compression test for each day of loading (days 1, 4, 7) (d_{max} = 50.8 mm)

The values of B_g for the dacite and andesite specimens after 1D compression testing under dry, wet and saturated conditions are presented in Table 8.

It can be seen in Table 8 that an increase in d_{max}

increased particle breakage in both types of material under all conditions. In dacite materials in the wet condition, there was less particle breakage when compared to the dry condition. In addition, particle breakage in the saturated tests increased slightly compared to the initial tests under dry and wet conditions. For the andesite specimens, there was less particle breakage in the dry tests compared to the wet tests. particle breakage increased slightly in the saturated tests compared to the initial tests under dry and wet conditions.

4.1.3 Particle breakage after Los Angeles tests

Fig. 9(a) shows the PSD curve for dacite and andesite specimens before and after Los Angeles testing. Fig. 9(b) shows the ΔW_k on different sieves for dacite and andesite specimens before and after Los Angeles tests.

Table 9 lists the values of B_g for both dacite and andesite specimens after Los Angeles testing. It can be seen that an increase in d_{max} increased particle breakage for both types of material.

4.2 Settlement of specimens

Fig. 10 shows the settlement diagram for dacite specimens under wet conditions and andesite specimens under dry conditions over the loading time. It is apparent that an increase in d_{max} increased settlement in both types of material under all conditions. There was a similar trend for the particle breakage test results.

Fig. 11 shows the settlement diagrams for dacite and andesite specimens under saturated conditions over the loading time. These conditions occurred after the initial loading steps and under both dry and wet conditions. It should be noted that a change in settlement is depicted only for the saturation step and that deformation was not significant after the wet tests, but higher after the dry tests.

Fig. 12 shows the daily deformation diagrams for 1, 4, and 7 day of loading under dry and wet conditions in order to study the daily settlement and deformation for every day of loading. The figures show that the greatest deformation occurred in the first hour. After 4 h of loading, deformation had increased slightly, but at the end of each loading time, the deformation was close to zero.

5. Discussion

Although previous studies and dam construction codes suggest mixing rockfill materials with a water content of 20%, the results of the new experiments show that it is better to compact some of the weak rockfill material used for the construction of dams under dry conditions (ICOLD 1993). As for the strong rockfill materials in both the specimen preparation stage and 1D compression tests, particle breakage parameters under dry conditions were either less than or greater than under wet conditions. The dacite materials, which had lower strength, showed more particle breakage under dry conditions than under wet conditions.

Andesite showed less particle breakage under dry conditions than under wet conditions. The difference in the behavior of these materials can be attributed to the presence of water in the rockfill materials and particle breakage mechanisms. The rockfill water content was significant and varied from zero to the saturation. The rockfill water content was significant and varied from zero to the saturation content of the rock particles and the dead water content at which the rockfill voids were filled (Oldecop and Alonso 2007). Fig. 13 shows that particle breakage was characterized by the mechanisms of angular fracture, particle cracking and particle breakup (Zhang *et al.* 2012b).

Fig. 13 Mechanisms of particle breakage: (1) angular fracture, (2) particle cracking and (3) particle breakup

During the specimen preparation stage for the dacite specimens, the greatest amount of water added under wet conditions was the significant water content. It functioned as a lubricant, reduced the surface friction, and facilitated the relative displacement of the particles of material. This, in turn, achieved the desired density with less breakage than for the dry tests. In the andesite specimens, the addition of the highest amount of water under wet conditions had the dead water content, which had no significant effect on surface friction. This made movement of the particles relative to each other difficult, because the amount of water absorbed by andesite and by the particles was low. Drainage did not occur during the preparation of specimens and the energy required to achieve the desired density for the sample increased as the amount of water increased. This increase in energy resulted in an increase in particle breakage in the andesite specimens under wet conditions over that in the dry conditions.

In the specimen preparation stage, angular fracture dominated the particle breakage mechanisms for the dacite and andesite materials. In the 1D compression tests, dacite primarily demonstrated the particle breakage mechanisms of angular fracture and particle breakup. The andesite primarily demonstrated angular fracture and particle cracking.

There were no remarkable changes in C_u and D_{50} in the PSD curves after the experiments, which indicates acceptable behavior of the tested materials with regard to the applied stress. Fig. 14 compares the particle breakage parameters in the specimen preparation phase and the 1D compression tests, for which Eq. (3) is proposed as:

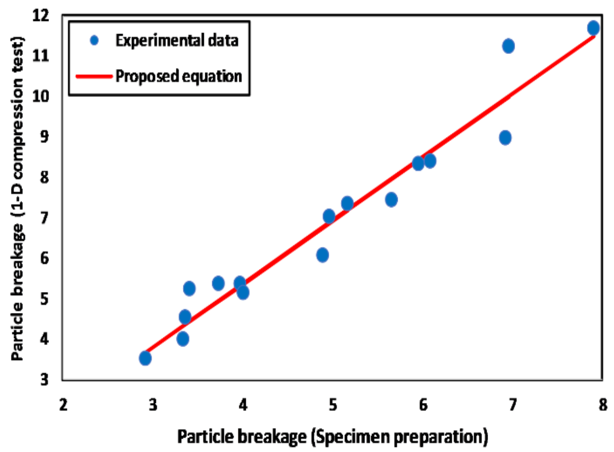

Fig. 14 Particle breakage in specimen preparation and 1D compression tests with different d_{max}

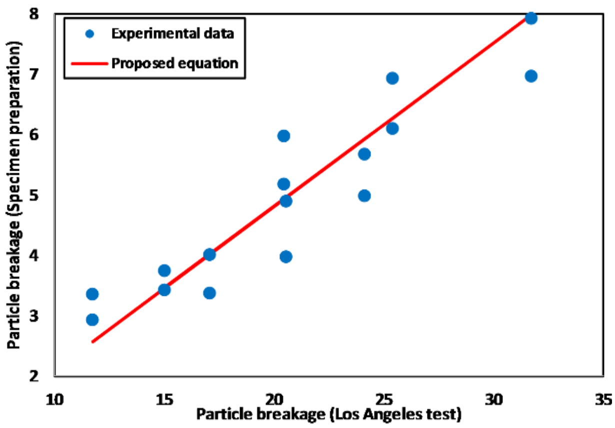

Fig. 15 Particle breakage in specimen preparation and Los Angeles tests with different d_{max}

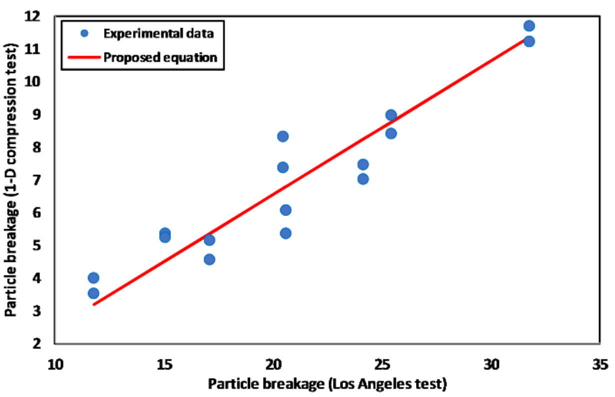

Fig. 16 Particle breakage in 1D compression and Los Angeles tests with different d_{max}

$$(B_g)_{1-D\ compression} = -0.903 + 1.566\ (B_g)_{compaction} \tag{3}$$

where $(B_g)_{compaction}$ is the particle breakage parameter during specimen preparation at d_{max} values greater than 2, $(B_g)_{1D\ compression}$ is the particle breakage parameter in the 1D compression tests for different values of d_{max} and R = 0.975 (correlation coefficient).

As a result of the increase in d_{max}, particle breakage increased for both types of material under all conditions. Eq. (4) has been proposed to determine the relationship between the particle breakage parameter and d_{max} in the 1D compression tests as:

$$(B_g)_d = 0.684 * \left(\frac{d}{d_0}\right) * (B_g)_{d_0} + 2.747 \tag{4}$$

where $d_0 =$ 50.8 cm, $(B_g)_{d_0}$ is the particle breakage parameter at d_{max} = 50.8 cm, d equals d_{max} in each test, $(B_g)_d$ is the particle breakage parameter in each test for different values of d_{max} and R = 0.924 (correlation coefficient).

Comparison of the results of the 1D compression and Los Angeles tests indicates that the particle shapes were different after testing; thus, the following equations are proposed to characterize the results of the two experiments.

For the results shown in Fig. 15, Eq. (5) is proposed for the particle breakage factor during specimen preparation and the Los Angeles tests:

$$(B_g)_{compaction} = -0.615 + 0.271\ (B_g)_{Los\ Angeles} \tag{5}$$

where $(B_g)_{Los\ Angeles}$ is the particle breakage parameter in the Los Angeles tests at d_{max} values greater than 10 and R = 0.965 (correlation coefficient).

For the results shown in Fig. 16, Eq. (6) is proposed for the particle breakage factor in the 1D compression and Los Angeles tests as:

$$(B_g)_{1-D\ compression} = -1.649 + 0.410\ (B_g)_{Los\ Angeles} \tag{6}$$

in which R = 0.966 (correlation coefficient).

In terms of settlement and strain, the specimens showed behavior that was similar to that of strong rockfill, in that the addition of water increased settlement. In the experiments conducted under dry conditions, deformation in the rockfill material was caused only by particle breakage during loading of the materials. However, particle breakage and the addition of water were the causes of deformation in the tests performed under wet conditions.

The results of the experiments indicated that the contribution of water to the deformation of dacite and andesite materials was 35% to 40%. Particle breakage in the materials was the causal factor for the occurrence of the remaining deformation. Settlement of the rockfill support shells in the construction stage should not exceed 1% to 3% of the height of dam (ICOLD 1993). The results of the experiments showed that the rockfill materials tested exhibited acceptable behavior at the construction stage under both wet and dry conditions. Furthermore, the effect of d_{max} on settlement was less for the dacite than the andesite specimens. This indicates that significant breakage occurred in the weaker materials at the specimen preparation stage and also in the 1D compression tests. Dacite material with different maximum size exhibited a similar trend with regard to settlement.

In the experiments conducted under saturated conditions, settlement was caused by an increase in the water content and time, of which the time factor on days 2-7 played a major role. About 70% to 80% of the settlement in the materials tested under saturated conditions were caused by an increase in the water content. The time factor contributed to the remaining 20% to 30% of deformation.

Settlement of the rockfill support shells in the operation stage of rockfill dams should not exceed 0.2% to 1% of the height of dam (ICOLD 1993). The results of the experiments showed that the settlement of the rockfill in both the construction and operation stages were acceptable for design purposes. In all experiments on materials having different maximum sizes, the settlement that occurred under saturation after the dry tests was greater than the deformations observed under saturation after the wet tests. This difference in the amount of settlement was more remarkable in the stronger rockfill material.

At each daily loading stage (24 h), increases in the load and the time resulted in settlement. The initial deformation occurring in the first hour was mainly caused by loading, while the time factor and rheological deformation contributed to deformations in the following hours. The results of the creep test on strong rockfill material after 24 h showed that 70% to 90% of deformation occurred within minutes of loading. The weak rockfill material displayed less-sudden settlement compared to that of the strong material under the same conditions. In other words, 70% to 80% of total deformation was caused by loading and the time factor and rheological factors contributed to the remaining 20% to 30% of deformation in each loading step. When the behavior of the tested materials is compared with the design criteria, it can be concluded that these rockfill materials are safe for use in construction of the dam body.

6. Conclusions

The behavior of weak rockfill materials and their applicability to dam construction has been investigated. One-dimensional (1D) compressional and Los Angeles tests were conducted on samples of weak rockfill material obtained from Nohob Dam in Qazvin, Iran and the effects of particle size and saturation conditions on their behavior was examined. The PSD curves for weak rockfill materials subjected to stress in the 1D compression tests was considered to be the index of evolution in the materials. The following conclusions could be drawn from the results:

• Weak rock showed acceptable behavior as rockfill in dam construction due to their low uniaxial compressive strength. particle breakage in the weak rockfill material was only slightly greater than in the strong rockfill material. Also, similar to the strong rockfill material, the increase in the particle size of the weak rockfill material increased the breakage factor.

• Particle breakage was characterized by the mechanisms of angular fracture, particle cracking and particle breakup. In the specimen preparation stage of the dacite and andesite materials, angular fracture dominated particle breakage. In the 1D compression tests, dacite material primarily demonstrated angular fracture and particle breakup as particle breakage mechanisms. The andesite materials primarily demonstrated angular fracture and particle cracking.

• The addition of water to the rockfill materials had the following functions: (a) As a lubricant that facilitates the relative displacement of particles. This function was more significant in weaker rockfill materials; (b) For absorption of energy by water during the compaction stage. This function was more significant in stronger rockfill materials, which were less porous and absorbed less water; (c) Softening of materials under stress after the addition of water. This function was more significant in weaker rockfill materials. In general, the behavior of the tested materials after the addition of water was appropriate. Moreover, in weak rockfill materials, the addition of water had no significant effect on particle breakage at all of the MPSs considered.

• Deformation in the tested rockfill materials was caused by particle breakage, the addition of water, the time factor and rheological deformation. Particle breakage played the major role in deformation of weak rockfill materials. Deformation in weaker rockfill material did not affect the MPS significantly, but was more notable in the stronger rockfill material.

• Comparison of particle breakage in the specimen preparation stage of the 1D compression and Los Angeles tests allowed development of the proposed equations with which to predict particle breakage at the specimen preparation stage and in 1D compression tests using the Los Angeles tests results for different MPS.

Acknowledgments

The authors would like to thank Mr. Mousavi and Mr. Keshavarz of the Qazvin Regional Water Company for their kind support and cooperation during the material sampling in this study.

References

Absaran Consulting Engineering (2010), *Nohob Storage Dam Studies*.

Araei, A.A., Razeghi, H.R., Ghalandarzadeh, A. and Tabatabaei, S.H. (2012), "Effects of loading rate and initial stress state on stress-strain behavior of rock fill materials under monotonic and cyclic loading conditions", *Scientia Iranica*, **19**(5), 1220-1235. https://doi.org/10.1016/j.scient.2012.08.002.

Araei, A.A., Tabatabaei, S.H. and Razeghi, H.R. (2012), "Cyclic and post-cyclic monotonic behavior of crushed conglomerate rockfill material under dry and saturated conditions", *Scientia Iranica*, **19**(1), 64-76. https://doi.org/10.1016/j.scient.2011.12.001.

ASTM C535 (2013), "Standard test method for resistance to degradation of large-size coarse aggregate by abrasion and impact in the Los Angeles machine", American Society for Testing and Materials, West Conshohocken, Pennsylvania, U.S.A.

ASTM D2216 (2010), "Standard test methods for laboratory determination of water (moisture) content of soil and rock by mass", American Society for Testing and Materials, West Conshohocken, Pennsylvania, U.S.A.

ASTM D4253 (2016), "Standard test methods for maximum index density and unit weight of soils using a vibratory table", American Society for Testing and Materials, West Conshohocken, Pennsylvania, U.S.A.

ASTM D4254 (2016), "Standard test methods for minimum index density and unit weight of soils and calculation relative density", American Society for Testing and Materials, West Conshohocken, Pennsylvania, U.S.A.

Ben-Nun, O. and Einav, I. (2010), "The role of self-organization during confined comminution of granular materials", *Philos. T. Royal Soc. A*, **368**(1910), 231-247. https://doi.org/10.1098/rsta.2009.0205.

Cetin, H., Laman, M. and Ertunc, A. (2000), "Settlement and slaking problems in the world's fourth largest rock-fill dam, the Ataturk Dam in Turkey", *Eng. Geol.*, **56**(3-4), 225-242. https://doi.org/10.1016/S0013-7952(99)00049-6.

Charles, J.A. and Watts, K.S. (1980), "The influence of confining pressure on the shear strength of compacted rockfill", *Geotechnique*, **30**(4), 353-367. https://doi.org/10.1680/geot.1980.30.4.353.

Cooke, J.B. (1984), "Progress in rockfill dams, (18th Terzaghi Lecture)", *Geotech. Eng.*, **110**(10), 1381-1414. https://doi.org/10.1061/(ASCE)07339410(1984)110:10(138-1).

Cooke, J.B. (1993), "Rockfill and the rockfill dam", *Proceedings of the International Symposium on High Earth-Rockfill Dams, Chinese Society for Hydro-electric Engineering*, Beijing, China, October.

Cristian, J. (2011), "Mechanical behavior of rockfill materials-Application to concrete face rockfill dams", Ph.D. Dissertation, Ecole Centrale Paris, Paris, France.

Einav, I., Houlsby, G.T. and Nguyen, G.D. (2007), "Coupled damage and plasticity models derived from energy and dissipation potentials", *Int. J. Solids Struct.*, **44**(7-8), 2487-2508. https://doi.org/10.1016/j.ijsolstr.2006.07.019.

Galloway, J.D. (1939), "The design of rock-fill dams", *Trans. Amer. Soc. Civ. Eng.*, **104**(1), 1-24.

Gupta, A.K. (2000), "Constitutive modelling of rockfill materials," Ph.D. Thesis, IIT, Delhi, India.

Gupta, A.K. (2009), "Effect of particle size and confining pressure on breakage and strength parameters of rockfill materials", *Elect. J. Geotech. Eng.*, **14**.

Gupta, A.K. (2009), "Triaxial behaviour of rockfill materials", *Elect. J. Geotech. Eng.*, **14**.

Gupta, A.K. (2016), "Effects of particle size and confining pressure on breakage factor of rockfill materials using medium triaxial test", *J. Rock Mech. Geotech. Eng.*, **8**(3), 378-388. https://doi.org/10.1016/j.jrmge.2015.12.005.

Hardin, B.O. (1985), "Crushing of soil particles", *J. Geotech. Eng.*, **111**(10), 1177-1192. https://doi.org/10.1061/(ASCE)07339410(1985)111:10(117-7).

Honkanadavar, N.P. and Sharma, K.G. (2016), "Modeling the triaxial behavior of riverbed and blasted quarried rockfill materials using hardening soil model", *J. Rock Mech. Geotech. Eng.*, **8**(3), 350-365. https://doi.org/10.1016/j.jrmge.2015.09.007.

ICOLD Bulletin134 (2008), *Weak Rocks and Shales in Dams*, International Commission on Large Dams, Paris, France.

ICOLD Bulletin92 (1993), *Rock Material for Rockfill Dams-Review and Recommendation*, International Commission on Large Dams, Paris, France.

Indraratna, B., Wijewardena, L.S.S. and Balasubramaniam, A.S. (1993), "Large-scale triaxial testing of greywacke rockfill", *Geotechnique*, **43**(1),37-51. https://doi.org/abs/10.1680/geot.1993.43.1.37.

ISRM (2000), *Suggested Methods for Determining the Uniaxial Compressive Strength and Deformability of Rock Materials*, International Society for Rock Mechanics, Lisbon, Portugal.

Khalkhali, A.B., Mirghasemi, A.A. and Mohammadi, S. (2011), "Numerical simulation of particle breakage of angular particles using combined DEM and FEM", *Powder Technol.*, **205**(1-3), 15-29. https://doi.org/10.1016/j.powtec.2010.07.034.

Lade, P.V., Yamamuro, J.A. and Bopp, P.A. (1996), "Significance of particle crushing in granular materials", *J. Geotech. Eng.*, **122**(4), 309-316. https://doi.org/10.1061/(ASCE)07339410(1996)122:4(309)

Lowe, J. (1964), "Shear strength of coarse embankment dam materials", *Proceedings of the 8th International Congress on Large Dams*, Paris, France, May.

Marachi, N.D., Chan, C.K. and Seed, H.B. (1972), "Evaluation of properties of rockfill material", *J. Soil Mech. Found. Div.*, **98**(1), 95-114.

Marsal, R J. (1967), "Large-scale testing of rockfill materials", *J. Soil Mech. Found. Div.*, **93**(2), 27-43.

Marsal, R.J. (1965), "Research on the behavior of granular materials and rockfill samples".

Miščević, P. and Vlastelica, G. (2009), "Shear strength of weathered soft rock-proposal of test method additions", *Proceedings of the Regional Symposium of ISRM–EUROCK 2009*, Cavtat, Croatia, October.

Miura, N. and Yamamoto, T. (1976), "Particle-crushing properties of sands under high stresses", *Technol. Reports Yamaguchi Univ.*, **1**(4), 439-447.

Miura, S., Yagi, K. and Asonuma, T. (2003), "Deformation-strength evaluation of crushable volcanic soils by laboratory and in-situ testing", *Soils Found.*, **43**(4), 47-57. https://doi.org/10.3208/sandf.43.4_47.

Nakata, Y., Kato, Y., Hyodo, M., Hyde, A.F. and Murata, H. (2001), "One-dimensional compression behaviour of uniformly graded sand related to single particle crushing strength", *Soils Found.*, **41**(2), 39-51. https://doi.org/10.3208/sandf.41.2_39.

Neves, D. Maranha, E. and Pinto, A.V. (1989), "Collapse of rockfill", *Proceedings of the 12th International Conference on Soil Mechanics and Foundation Engineering*, Rio de Janeiro, Brazil, August.

Neves, D. Maranha, E. and Veiga Pinto, A. (1988), "Modelling collapse on rockfill dams", *Comput. Geotech.*, **6**(2), 131-153. https://doi.org/10.1016/0266-352X(88)90077-8.

Nishiyama, T., Murakami, A., Chihara, E. and Hasegawa, T. (2006), "A study to estimate the deterioration of rockfill materials", *Proceeding of the International Symposium on Geomechanics and Geotechnics of Particulate Media*, Ube, Japan, September.

Nobari, E.S. and Duncan, J.M. (1972), "Effect of reservoir filling on stresses and movement in Earth and rockfill dams", A Report of an Investigation (No. TE-72-1), University of California, Berkeley, California, U.S.A.

Oldecop, L.A. and Alonso, E.E. (2007), "Theoretical investigation of the time-dependent behaviour of rockfill", *Geotechnique*, **57**(3), 289-301. https://doi.org/10.1680/geot.2007.57.3.289.

Parkin, A.K. (1977), "The compression of rockfill", *Australian Geomech. J.*, **7**, 33-39.

Sayao, A.S.F.J., Maia, P.C.A. and Nunes, A.L.L.S. (2005), "Considerations on the shear strength behavior of weathered rockfill", *Proceedings of the 16th International Conference on Soil Mechanics and Geotechnical Engineering*, Osaka, Japan, September.

Sherard, J.L. and Cooke, J.B. (1987), "Concrete-face rockfill dam: I. Assessment", *J. Geotech. Eng.*, **113**(10), 1096-1112. https://doi.org/10.1061/(ASCE)0733-9410(1987)113:10(1096).

Sowers, G.F. (1965), "Compressibility of broken rock and the settlement of rockfills", *Proceedings of the 6th International Conference on Soil Mechanics and Foundation Engineering*, Montreal, Canada, September.

Varadarajan, A., Sharma, K.G., Venkatachalam, K. and Gupta, A.K. (2003), "Testing and modeling two rockfill materials", *J. Geotech. Geoenviron. Eng.*, **129**(3), 206-218. https://doi.org/10.1061/(ASCE)1090-0241(2003)129:3(206).

Vasistha, Y., Gupta, A.K. and Kanwar, V. (2012), "Prediction of shear strength parameters: Of two rockfill materials", *Elect. J.*

Geotech. *Eng*.
Vasistha, Y., Gupta, A.K. and Kanwar, V., (2013), "Medium triaxial testing of some rockfill materials", *Elect*. *J*. *Geotech*. *Eng*., **18**.
Wang, T., Liu, S. and Lu, Y. (2019), "Laboratory experiments on the improvement of rockfill materials with composite grout", *Geomech*. *Eng*., **17**(3), 309-318. https://doi.org/10.12989/gae.2019.17.3.307.
Woo, I., Fleurisson, J.A. and Park, H.J. (2010), "Influence of weathering on shear strength of joints in a porphyritic granite rock mass in Jechon area, South Korea", *Geosci*. *J*., **14**(3), 289-299. https://doi.org/10.1007/s12303-010-0026-0.
Xiao, Y. and Liu, H. (2017), "Elastoplastic constitutive model for rockfill materials considering particle breakage", *Int*. *J*. *Geomech*., **17**(1),4016041. https://doi.org/10.1061/(ASCE)GM.1943-5622.0000681.
Xiao, Y., Liu, H., Chen, Y. and Jiang, J. (2014), "Strength and deformation of rockfill material based on large-scale triaxial compression tests. II: Influence of particle breakage", *J*. *Geotech*. *Geoenviron*. *Eng*., **140**(12), 4014071. https://doi.org/10.1061/(ASCE)GT.1943-5606.0001177
Xiao, Y., Liu, H., Zhang, W., Liu, H., Yin, F. and Wang, Y. (2016), "Testing and modeling of rockfill materials: A review", *J*. *Rock Mech*. *Geotech*. *Eng*., **8**(3),415-422. https://doi.org/10.1016/j.jrmge.2015.09.009.
Xiao, Y., Meng, M., Daouadji, A., Chen, Q., Wu, Z. and Jiang, X. (2018), "Effects of particle size on crushing and deformation behaviors of rockfill materials", *Geosci*. *Front*., **11**(2), 375-388. https://doi.org/10.1016/j.gsf.2018.10.010.
Yamamuro, J.A., Bopp, P.A. and Lade, P.V., (1996), "One-dimensional compression of sands at high pressures", *J*. *Geotech*. *Eng*., **122**(2), 147-154. https://doi.org/10.1061/(ASCE)0733-9410(1996)122:2(147).
Yin, Y., Zhang, B.Y., Zhang, J.H. and Sun, G.L. (2016), "Effect of densification on shear strength behavior of argillaceous siltstone subjected to variations in weathering-related physical and mechanical conditions", *Eng*. *Geol*., **208**, 63-68. https://doi.org/10.1016/j.enggeo.2016.04.028.
Zhang, B.Y., Zhang, J.H. and Sun, G.L. (2012), "Particle breakage of argillaceous siltstone subjected to stresses and weathering", *Eng*. *Geol*., **137**, 21-28. https://doi.org/10.1016/j.enggeo.2012.03.009.
Zhang, B.Y., Zhang, J.H. and Sun, G.L. (2015), "Deformation and shear strength of rockfill materials composed of soft siltstones subjected to stress, cyclical drying/wetting and temperature variations", *Eng*. *Geol*., **190**, 87-97. https://doi.org/10.1016/j.enggeo.2015.03.006.

GC